

Social 3D Scene Graphs: Modeling Human Actions and Relations for Interactive Service Robots

Ermanno Bartoli^{1*} Dennis Rotondi^{2*} Buwei He¹ Patric Jensfelt¹ Kai O. Arras^{2†} Iolanda Leite^{1†}

Abstract—Understanding how people interact with their surroundings and each other is essential for enabling robots to act in socially compliant and context-aware ways. While 3D Scene Graphs have emerged as a powerful semantic representation for scene understanding, existing approaches largely ignore humans in the scene, also due to the lack of annotated human-environment relationships. Moreover, existing methods typically capture only open-vocabulary relations from single image frames, which limits their ability to model long-range interactions beyond the observed content. We introduce Social 3D Scene Graphs, an augmented 3D Scene Graph representation that captures humans, their attributes, activities and relationships in the environment, both local and remote, using an open-vocabulary framework. Furthermore, we introduce a new benchmark consisting of synthetic environments with comprehensive human–scene relationship annotations and diverse types of queries for evaluating social scene understanding in 3D. The experiments demonstrate that our representation improves human activity prediction and reasoning about human–environment relations, paving the way toward socially intelligent robots.

I. INTRODUCTION

Service robots are increasingly being deployed in human-centric environments such as homes and offices. In order to be effective in such spaces, they need more than just metric representations [1]. They must also understand how humans interact with their surroundings and reason what these interactions entail, e.g., for providing the right service at the right time. For example, a person sitting on a sofa and watching television defines a leisure zone where the robot should avoid blocking the view. A person at a dining table with an empty glass creates a meal context where the robot should infer the need for water rather than beginning to clean. Social robots must be able to accurately interpret such situational cues, to achieve socially compliant, anticipatory, and context-aware behavior.

3D Scene Graphs (3DSGs) [2], [3] offer a promising environment representation for robots to achieve these goals. They have recently gained popularity in the robotics community as a semantic representation for scene understanding and downstream tasks, due to their ability to compactly encode rich 3D information [4] and their versatility in a wide

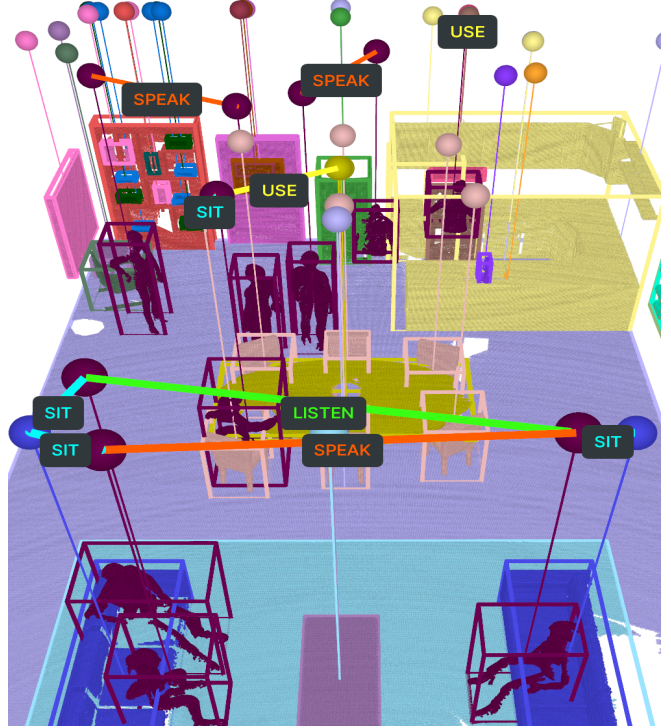


Fig. 1: Example of a Social 3D Scene Graph. Each entity is represented as a node in the graph and visualized as a sphere. These nodes are connected by social edges (e.g., **SPEAK** and **LISTEN**) that capture their activities in the scene.

range of applications. However, a major limitation of current 3DSG approaches is the absence of human relationships within the 3D environments where they are deployed (e.g., [5]–[9]). This is largely due to the scarcity of annotated data capturing human–environment relationships, which led researchers to use non-public datasets for evaluating their methods involving humans [10]. In addition, state-of-the-art 3DSG methods typically capture open-vocabulary spatial relationships only at a local level, extracting them from a single view by prompting a vision-language model (VLM) or by comparing 3D features such as embeddings or occupied volume. Yet, humans frequently interact with objects or other people across larger spatial extents, beyond the scope of a single frame¹, making standard 3DSG construction algorithms unsuited for modeling such interactions.

Motivated by these challenges, we address the problem of

*Equal contribution.

†Equal supervision.

¹E. Bartoli, B. He, P. Jensfelt and I. Leite are with Faculty of Robotics Perception and Learning, KTH Royal Institute of Technology, Stockholm, Sweden. Email: bartoli@kth.se

²D. Rotondi and K.O. Arras are with the Socially Intelligent Robotics Lab, Institute for Artificial Intelligence, University of Stuttgart, Germany. Email: dennis.rotondi@ki.uni-stuttgart.de

¹Note that in this work, we define a single frame as an RGB image captured using a pinhole camera model, following the standard in the field.

generating Social 3D Scene Graphs (S3DSG), i.e., 3DSGs that model human activities and their relationships with the environment beyond local single-frame interactions, by assuming that humans look at the objects they engage with (see Fig. 1). Specifically, our contributions are:

- We introduce Social 3D Scene Graphs and propose a method to build them, augmenting 3DSGs with humans’ relationships and activities through our ReaSoN module, which operates in open-vocabulary settings.
- We introduce a benchmark, SocialGraph3D, to evaluate human relationships, activities and social scene understanding in 3D.
- We use our benchmark to demonstrate that our representation outperform state-of-the-art performance on the introduced tasks, and we qualitatively show how S3DSG can be applied to a real-world downstream task.

We open-source our code and dataset upon acceptance at the link: <https://github.com/anonymous/social3dsg>.

II. RELATED WORK

A. 3D Scene Graphs

Armeni et al. [2] introduced the concept of 3D Scene Graphs, $\mathcal{G} = (\mathcal{V}, \mathcal{E})$, a hierarchical structure built over a 3D representation such as a mesh or point cloud, in which nodes \mathcal{V} represent objects and spatial entities (e.g., rooms, floors, buildings), and edges \mathcal{E} capture relationships between them, including spatial (e.g., A “on top of” B), comparative (e.g., A “smaller than” B), and support (e.g., A “standing on” B).

Follow-up works [11]–[15] aimed to construct such representations from sets of registered RGB-D images. However, these methods focus solely on spatial relationships between places and on relations that can be inferred from a single image (requiring the objects to appear in the same frame) using a VLM, without incorporating humans into the representation.

In parallel, the vision community has explored the task of predicting 3D semantic scene graphs [16]–[20] from class-agnostic segmented point clouds, framing it as a classification problem typically addressed using iterative message-passing schemes [21] with graph neural networks, which however suffer from the vanishing gradient problem [22] and therefore often restrict the number of iterations, limiting their ability to capture long-range relationships. While the predicted relationships are generally not constrained to the locality of a single image frame, these approaches focus solely on 3D features and are trained on the 3DSSG dataset [16], which, like the dataset from [2], is limited to close vocabulary object-centric relationships.

Zhang et al. [9] introduce the dichotomy of local and remote relationships and take an initial step toward addressing open-vocabulary remote functional relationships by proposing a confidence-aware reasoning approach. This method leverages the commonsense knowledge of a large language model to infer links between functionally related but spatially distant objects, such as a light switch and the light it controls. However, their framework remains object-centric, focusing solely on functional relations and entirely neglecting humans.

B. Humans in 3D Scene Graphs

Motivated by the need to track agents in a scene, 3D Dynamic Scene Graphs [10], [23], [24] model the temporal evolution of human poses as nodes and generate mesh representations of them; however, they capture only relationships between places and pairwise spatio-temporal relations (e.g., “agent A is in room B at time t”). The data in these works come from a Unity simulator, but most resources, such as the semantic mesh, are not publicly available. In contrast, our work builds and publicly releases scenes with synthetically generated humans, complete with full annotations.

Building on 3D dynamic scene graphs, the work most closely related to ours is that of Gorlo et al. [25], who tackle the problem of estimating human trajectories in complex environments by reasoning about human-scene interactions. In their approach, however, interactions with the environment are used solely to model how individuals navigate their surroundings. Furthermore, their method makes the strong assumption that only a single person is present in the scene, thereby excluding by design all interactions between people. In contrast, we explicitly model such interactions, which we consider crucial for a robot’s contextual understanding: for example, recognizing that it should not disturb people who are engaged in conversation.

C. Planning with 3D Scene Graphs

3DSGs are well-suited for robot navigation, task planning, and motion planning because they provide topological environment models that are easily compatible with classical PDDL solvers [26], [27] and can support reasoning with LLMs [28], [29]. For example, consider the task: “A postdoc spilled their soda. Help them clean it up.” used in [28], where such queries are employed for planning. In contrast, our goal is to embed this knowledge directly into the representation: by explicitly modeling entities such as the postdoc and the soda, the representation enables an LLM to reason about the situation, for example, by deciding whether to avoid the spill or clean it up.

Additionally, 3DSGs have proven effective for grounding navigation goals expressed in unconstrained natural language [30], [31]. By modeling social relationships, it becomes possible to incorporate costs and clearance into the navigation process, enabling socially aware behaviors such as avoiding passing in front of people watching TV.

We share similar goals with the field of social robot navigation, which focuses on learning motion behaviors for human environments that are safe, efficient, and considered socially acceptable [32]. Examples include group-aware avoidance behaviors that use a *social graph* whose edge costs are learned to encode group affiliation [33], approach behaviors to groups of humans for multi-party interaction [34], or predictive motion planning in dense crowds [35]. While these works can cope with dynamic scenes, they are typically constrained to motion behavior in 2D with limited social and semantic scene understanding. Our 3DSG approach aims to support such tasks with rich 3D semantic

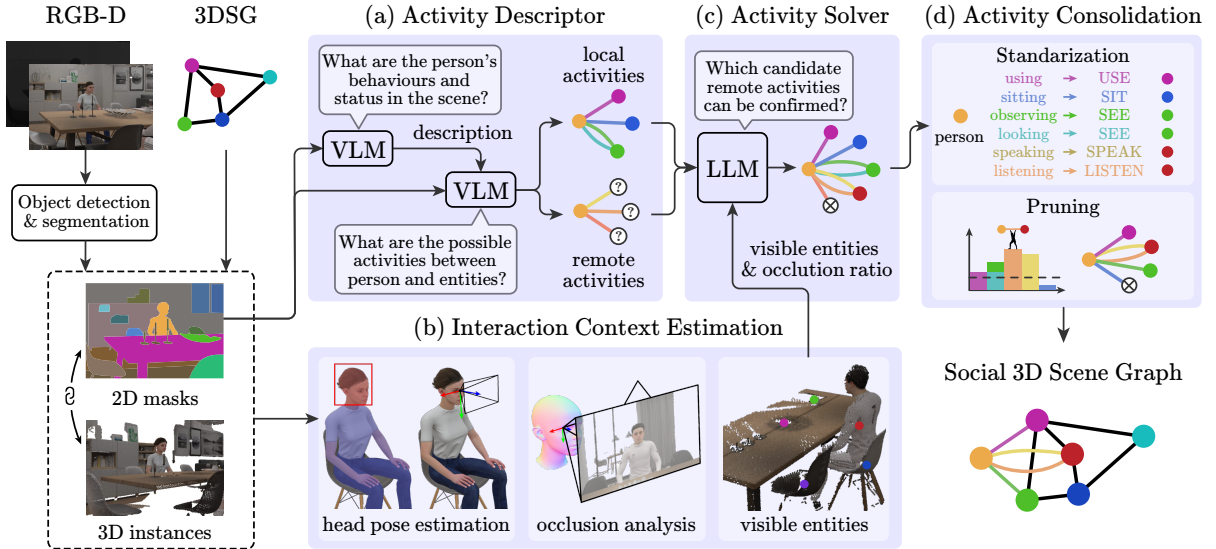


Fig. 2: An overview of our solution ReaSoN, which extends existing 3D Scene Graphs with humans and their activities through four key components: (a) **Activity Descriptor** segments humans and generates behavior descriptions using VLMs, and identifies both local and remote activities under the context; (b) **Interaction Context Estimator** estimates head pose and models each person’s visible frustum to determine visible entities through occlusion analysis; (c) **Activity Solver** uses LLM spatial reasoning to validate remote activities by finding relevant entities; and (d) **Activity Consolidation** refines activities using semantic frames and prunes spurious detections based on frequency thresholds, producing a robust Social 3DSG.

representations and enabling human-centric reasoning and queries.

III. METHOD

A. Problem Formulation

Our objective is to build Social 3D Scene Graphs, enabling robots to understand and operate in human-centric environments more effectively. We define a Social 3D Scene Graph as an extension of a traditional 3D Scene Graph that incorporates nodes and edges representing humans and their activities in addition to objects and spatial relationships. Formally, a Social 3D Scene Graph is represented as a tuple $\mathcal{G} = (\mathcal{V}, \mathcal{E})$ where:

- $\mathcal{V} = \mathcal{V}_o \cup \mathcal{V}_h$ is the set of nodes, where \mathcal{V}_o represents objects and \mathcal{V}_h represents humans in the environment.
- $\mathcal{E} = \mathcal{E}_s \cup \mathcal{E}_a$ is the set of edges, where \mathcal{E}_s represents spatial relationships and \mathcal{E}_a represents activity relationships (e.g., “sitting”, “talking to”, “looking at”).

Our goal is not to reconstruct the complete 3D representation of the environment, but rather to incorporate humans and their activities into an existing 3DSG \mathcal{SG} . We assume the availability of \mathcal{SG} for an environment (without human representations), grounded to a 3D point cloud and derivable using methods such as ConceptGraphs [13]. The challenge lies in accurately detecting humans, estimating their interaction field, and inferring their activities from a sequence of registered RGB-D observations $\mathcal{I} = \{I_1, I_2, \dots, I_n\}$ of the same scene and coordinate system of \mathcal{SG} . We assume that in these images, the humans remain still except for facial expressions and mouth movements. We believe this approach is particularly relevant for service robots operating in human environments, where the primary sources of change are the

humans and their activities, the surroundings remain static and objects are assumed not to move. However, by handling the reconstruction and processing of humans at the final stage of a 3D Scene Graph generation pipeline, our approach can be seamlessly integrated into existing systems. We refer to our solution as the ReaSoN module.

B. RElationship and SOcial reasoNing in 3D

In this section, we describe how our module “RElationship and SOcial reasoNing in 3D” (ReaSoN) augments a 3D Scene Graph with human-related information to construct Social 3D Scene Graphs. As illustrated in Fig. 2, ReaSoN is composed of four submodules and activates whenever at least one human is detected. The pipeline processes each RGB-D observation $I_k \in \mathcal{I}$ by (i) detecting objects and humans (collectively referred to as entities), (ii) aligning detected objects with existing nodes in \mathcal{SG} , and (iii) estimating their activities through an understanding of fields of view, body pose, and socially relevant attributes. The resulting graph is an augmented version of \mathcal{SG} that explicitly encodes human behaviors and interactions.

Activity Descriptor. This module takes the entity detections as input and generates candidate descriptions of human behaviors along with their potential relationships. Human bounding boxes are used as prompts for a segmentation model to generate masks. We then apply morphological dilation to the resulting masks to highlight the contours and visually label the people in the image with their respective IDs and markers. As shown in [36], the markers enhance the generalization ability of the VLM, which analyzes the annotated image and outputs, for each human, a detailed characterization of their behaviors, including *posture* (e.g.,

upright, leaning), *gaze* (e.g., direct, averted), *physical state* (e.g., standing, sitting), and other socially relevant attributes. We then re-annotate the original input image I_k , labeling not only the humans but also all detected objects in the scene. The VLM takes as input the newly annotated image and the behavior descriptions from the previous step, and infers the activities the humans are or might be performing. This process yields two sets of relationships:

- *Local activities*: activities for which the relevant object or person involved is present in the image, allowing the VLM to confidently confirm their occurrence.
- *Remote activities*: activities that might be inferred from the behavior description and the image, but cannot be confidently confirmed due to insufficient context (e.g., the relevant object or person is outside the image).

Interaction Context Estimator. The interaction context estimator is introduced to determine the entities visible from a person’s perspective, thereby enabling the understanding of remote activities beyond the directly observable field of view of a single image. The estimator focuses on two key aspects: (i) head pose estimation, used to approximate each person’s visual perceptual field, and (ii) occlusion analysis, which identifies the visually perceivable entities for each person along with their occlusion ratios.

For head pose estimation, we employ a two-stage strategy: person heads are first localized using a pre-trained detector, after which their full-range 3D orientations are estimated with a pre-trained model, and the head centroid is obtained from the depth image to anchor orientation in 3D space.

Given the estimated head pose, we simulate the visual frustum for each person and conduct visibility analysis. Scene entities are rendered in the person’s view as depth images. To mitigate missing regions in the projected point clouds, we capture the silhouette of each entity and interpolate depth values within its boundary, thereby constructing a dense depth proxy. Occlusions are then resolved by depth comparisons across entities. For each entity, we compute the proportion of its projected area that remains visible from the person’s perspective, quantified by the silhouette occlusion index in [37].

Activity Solver. The central objective here is to identify the entities with which to establish relationships within the set of visible ones, validating remote activities through the emerging spatial reasoning capabilities of LLMs [38]. For a set of remote activities identified as requiring disambiguation and their human behavior descriptions provided by the Activity Descriptor, the Activity Solver inspects the partial 3D scene graph that includes the entities within the human’s field of view to locate relevant entities. For example, if a person appears to be reading but no book is directly visible, the VLM searches for plausible reading materials within the interaction space, taking into account the visible entities and their occlusion ratio from each person’s view, and typical reading distances.

Activity consolidation. After all images are processed, activity consolidation finalizes the Social 3D Scene Graph by refining activities for coherence and robustness. For each

human-entity pair connected by at least one edge, we ensure that all activity labels are clustered within augmented semantic frames that capture the full range of linguistic synset variation [39], [40]. For example, for the pair (Person1, Person2), activities such as “chatting with,” “speaking to,” and “talking to” are all canonicalized under the semantic frame SPEAK. This consolidation ensures that a single, consistent representation is used for each unique activity type throughout the 3D Scene Graph, while preserving the open-vocabulary capabilities of the method. We keep track of the number of activities clustered in each frame, which informs the subsequent pruning step. To minimize errors in the pipeline, such as visual ambiguities, particularly within the Activity Descriptor module, we prune activities based on their detection frequency. The key idea is that correct activities will appear more consistently across observations than spurious ones.

An edge $e \in \mathcal{E}$ is retained only if its detection count $N(e)$ satisfies both relative and absolute thresholds:

$$\text{Keep}(e) \iff N(e) \geq \max(\tau \cdot M, N_{\min}) \quad (1)$$

where $M = \max_{e'} N(e')$ is the maximum count among edges from the same node, $\tau \in (0, 1]$ is a relative threshold, and N_{\min} is an absolute cutoff. In short, edges are kept only if they occur frequently relative to the most common activity and exceed a minimum support level, effectively removing spurious detections.

C. Implementation

We set $\tau = 0.4$, and $N_{\min} = 2$. As a general-purpose detector, we used YOLO-World-V2 [41]; for segmentation, SAM2 [42]; for head localization, SSD MobileNet [43]; for 3D head orientation estimation, 6DRepNet360 [44]; and for both VLM and LLM components, GPT-5 [45]. The same model configuration was employed throughout all runs.

IV. EXPERIMENTS

Our experiments quantitatively evaluate the accuracy of ReaSoN in predicting human activities in 3D environments, its applicability to 3D social scene understanding, and qualitatively assess its use in a real-world application. We rely on our newly created benchmark, which includes human activities and is designed to assess models on human-centric reasoning and queries. We finally showcase its application in a navigation task.

A. SocialGraph3D Benchmark

As discussed in Sec. II-A, existing 3DSG datasets focus on environments without humans, leaving a gap in representing people and their interactions. To address this, we introduce the *SocialGraph3D* benchmark, comprising 8 synthetic home environments built in Unity, each with 3 to 9 inhabitants manually placed to interact with one another and with objects. The humans here are static but display facial movements that allow the detection of activities such as speaking. For each scene, we provide ground-truth point clouds and registered RGB-D images, each paired with a ground-truth

Information	Count
Total Unique Humans	42
Total Relationships (GT)	110
Query Distribution	
Total Activity Queries	38
Total Functional Queries	26
Total Spatial Queries	16
Activity Type Distribution	
Total Unique Activity Types	11
Activities: COOK, INTERACT, LIE, LISTEN, READ, REST, SEE, SIT, SPEAK, STAND, USE	

TABLE I: Aggregate information for the SocialGraph3D benchmark. All the relationship frames used are reported.

semantic mask of the objects in the scene. In addition, every scene includes a file listing all relationships among human instances and containing queries about the people in the scene, along with the corresponding instance IDs that satisfy them. Taken together, this constitutes our benchmark. Further details are provided in Tab. I. The ground-truth relationships annotation process is defined in Sec. IV-B and queries on the map have been detailed in Sec. IV-C.

B. Activity Relationships Prediction

In the following, we both describe how we generated the ground truth (GT) for human activities in the scenes adopting a human-in-the-loop methodology, and how we evaluated ReaSoN against two baselines. As the first baseline, we utilized ConceptGraphH (CGH), our extension of ConceptGraphs for detecting human activity, enabling the VLM prompt to relate humans with the other entities. As a second baseline, we consider ReaSoN without generating the behavior description in a separate step, but rather together with the step of proposing relationships, which we refer to as ReaSoN_{w/o BD}. Since ReaSoN requires multiple forward passes of the VLM, we wanted to justify the additional computation in contrast to a simpler approach. As input to ReaSoN and ReaSoN_{w/o BD}, we use our benchmark registered RGB-D images and a 3DSG generated by the standard (without humans) ConceptGraphs pipeline. CGH input is the registered RGB-D images.

We generated an initial set of activity predictions for each person in the scenes using the two main methods: ReaSoN and CGH. Next, we recruited 20 expert human evaluators, divided into two groups of 10 (one per model), to assess the plausibility of the generated activities. For each person in a scene, evaluators were shown multiple viewpoints and asked to rate each predicted activity on a scale from 1 (“Not reasonable at all”) to 5 (“Highly reasonable”). On average, CGH produced 5.38 activities per scene, while ReaSoN produced 17.75. They were also provided with an open-ended form to suggest any activities they felt were missing. We applied a median split to the activity ratings, retaining only predictions with an average score above the 50th percentile, which corresponded to a threshold of 4.33. For the open-ended suggestions, an activity was included

Map	CGH			ReaSoN _{w/o BD}			ReaSoN (ours)		
	P	R	F1	P	R	F1	P	R	F1
Map1	66.7	25.0	36.4	0.0	0.0	0.0	57.1	75.0	64.9
Map2	80.0	26.7	40.0	35.7	33.3	34.5	44.4	80.0	57.1
Map3	80.0	25.0	38.1	80.0	25.0	38.1	61.1	68.8	64.7
Map4	42.9	23.1	30.0	58.3	53.9	56.0	60.0	69.2	64.3
Map5	100.0	42.9	60.0	57.1	57.1	57.1	71.4	71.4	71.4
Map6	50.0	16.7	25.0	29.6	44.4	35.6	57.7	83.3	68.2
Map7	0.0	0.0	0.0	66.7	33.3	44.4	50.0	83.3	62.5
Map8	60.0	17.6	27.3	53.9	41.2	46.7	70.0	82.4	75.7
Total	60.0	22.2	32.4	45.7	34.3	39.2	57.6	76.9	65.9

TABLE II: Relationship prediction results on all the SocialGraph3D maps. Reported as percentages of Precision (P), Recall (R), and F1-Score.

in the GT if at least 30% of evaluators proposed it. The final GT is thus the union of these filtered predictions and consistently suggested activities, which results in a total of 110 relationships. Among the open-ended suggestions of the CGH group, there were all the relationships proposed by ReaSoN.

Building on this, we evaluated all three models’ performance in predicting human activities by comparing the outputs with the GT using precision, recall, and F1-score metrics. A prediction was considered a true positive if it had at least 10% intersection-over-union (IoU) with the ground-truth point clouds of the related objects, matched the ground-truth label, and its relationship label belonged to the same semantic frame [39]. Results are reported in Tab. II.

Although ReaSoN achieves the highest overall F1-score, it does not outperform across all metrics. Indeed, CGH obtains higher precision, but this advantage reflects a conservative prediction style, focusing only on a few high-confidence activities while overlooking many valid interactions. Such behavior highlights the model’s lack of a mechanism to identify a broader range of relationships outside the single image frame. As a result, CGH captures only a total of 43 activities across 6 frames, capturing a small fraction of the true activities, with READ being the only frame it detects exclusively. In contrast, ReaSoN predicts 142 activities across 10 frames (see Tab. I), and increasing coverage by nearly 50%. Notably, ReaSoN identifies frames such as INTERACT, LISTEN, REST, SPEAK, STAND, USE, none of which are ever detected by CGH.

ReaSoN_{w/o BD} also predicts a larger activity space, with 81 activities across the same 10 frames as ReaSoN, but its performance is consistently weaker. In particular, ReaSoN_{w/o BD} struggles with activities requiring contextual reasoning beyond immediate visual cues. For example, in a cluttered scene where a person’s direct line of sight to an object is partially obscured, ReaSoN can still infer a USE relationship by leveraging the broader context encoded in the behavior description. In contrast, ReaSoN_{w/o BD} is more likely to miss such subtle interactions, as it loses important details about the person’s focus and intent when processing a cluttered annotated image in a single pass.

This illustrates that the single-step behavior description

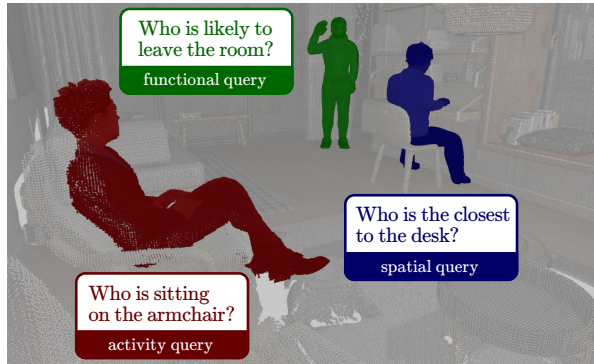


Fig. 3: Illustrative example from our Social Scene Understanding benchmark: queries and their corresponding 3D answers from our method are shown in the same color. From top to bottom, their type is *functional* (green), *spatial* (blue), and *activity* (red).

is a crucial component of our model, as it helps the system avoid hallucinations and identify distant activities. We conclude that when using a cluttered annotated image, the model loses important details about people that are needed at different stages of the pipeline.

C. Social Scene Understanding

We designed a set of questions to evaluate the ability of our representation to support 3D social scene understanding, i.e., given an input 3D scene representation and a natural language query about the scene involving human activities and interactions, the task is to detect the corresponding human instance in the representation (see Fig. 3). The queries are divided into three categories of increasing complexity:

- **Spatial queries** focus on spatial relationships between humans and objects, such as “Who is the closest to the lamp?” or “Who is next to the window?”.
- **Activity queries** involve combining spatial relationships with human activity understanding, such as “Who is watching TV on the bed?”.
- **Functional queries** involve spatial relationships, human activities, and commonsense reasoning, such as “Who is likely to want to eat some food?”. Answering such questions requires the model to infer, for example, that a person sitting at the table while watching someone cook is likely to want to eat soon.

We have a total of 80 queries across 8 scenes, with 105 points obtainable in total, one for each correct instance retrieved. For each query, the correct solution contains at most two instances, as we are also interested in capturing activities between pairs of people. As query complexity increases, the solution must integrate more information from the Social 3D Scene Graph and perform more advanced reasoning. We evaluate the ability to retrieve the correct person, given a query, using two different feature-based baselines: CLIP_ALL, which compares the CLIP [46] features of the query with those of all the objects in the graph (as is standard in 3DSG sota methods [12]–[14]), and outputs the most likely match. To reduce the search space and assess how

Method	Spatial	Activity	Functional	Mean	Pts
CGH	46.4	44.6	41.5	44.2	47
CLIP_FAV	64.3	52.1	55.1	57.2	57
CLIP_ALL	31.0	24.6	25.1	26.9	29
ReaSoN (ours)	79.8	81.9	64.6	75.4	81

TABLE III: Social scene understanding results per query type. Reported as the ratio (%) between the collected points (Pts) and the total points.

much can be captured with purely visual observations, we also use CLIP_FAV, which follows the same CLIP approach but restricts the comparison to the multimodal features of human nodes only.

We moreover compare our method with the LLM reasoning approach of ConceptGraphs, adapted to our CGH output. This solution consists of feeding the LLM with a detailed JSON description of the nodes and the relationships between them. We find this approach inefficient and contrary to the principle of maintaining a lightweight representation that the LLM can parse effectively in order to perform the complex reasoning required to answer functional queries. For this reason, we developed our own JSON format of the Social 3DSG, which is then provided to the LLM together with the query. Each node is represented as [id, class, 3D center], and each edge as [id_from, id_to, relationship_frame], thereby removing the additional edge descriptions and object tags used in the baselines. However, our representation does not lose this level of detail, since we also associate with the graph a compact JSON containing the frame description, gloss, and example actions provided by the inventory [39]: one for each unique relationship frame in the graph. For example: [SEE; An experiencer SEES a stimulus in favour of a beneficiary; Perceive by sight or have the power to perceive by sight; Watch, see, observe]. For feature-based methods, we retrieve the top-2 most likely nodes if the query requires two results, while for the LLM parsing approach, we compare the GT with at most the top-2 candidate results. We assign one point for each correctly retrieved human in the GT if the retrieved method has an $\text{IoU} \geq 0.10$, and then compute the ratio between obtained points and total possible points. We report the results by query type in Tab. III.

This experiment makes it clear that, unlike in object-based queries, feature-based solutions are not well-suited for processing large 3DSGs to handle complex human-centered queries. They perform the worst, mainly because the bag-of-words effect often shifts the focus toward the objects mentioned in the query, even when only a small number of humans are involved. They can find the correct answer when the object mentioned in the query is close to the mask into which it has been embedded. This occurs most often for spatial queries, but when the task requires processing more remote relationships, their limitations become evident. From the scores, we also observe that our more

compact representation not only helps in processing activity relationships required to answer queries, but also enables more effective reasoning for spatial queries. By reducing the number of tokens, it prevents context window overflow that can cause LLMs to lose track of relevant information, thereby demonstrating the superiority of our serialization.

D. Application in a Downstream Task

As a final experiment to qualitatively validate the practical utility of ReaSoN in a real-world downstream task, we conducted a navigation experiment in a novel scene with RGB-D data captured using an iPhone 15 Pro (30 FPS, downsampled to 5 FPS). The scene was staged to depict a common social situation: two people engaged in conversation.

We integrate ReaSoN into a 3DSG pipeline, generating both a 3D instance-segmented point cloud of the environment and the corresponding Social 3D Scene Graph. This reconstructed map was then provided to a sample-based motion planner [47], which produced a conventionally cost-optimal (shortest) trajectory from a start to a goal position; visualized as the blue path in Fig. 4. Next, we leverage the Social 3D Scene Graph for socially-aware motion planning by augmenting the geometric cost map with a “social cost”. Specifically, interactions such as the identified SPEAK relationship create a high social-cost region between the two individuals (visualized in the lower layer of Fig. 4). This field penalizes paths that intersect the interaction space, with the cost at any point p calculated as:

$$C_{\text{social}}(p) = \begin{cases} C_{\text{rel}} \times \left(1 - \frac{d(p, L_{ij})}{R}\right) & \text{if } d(p, L_{ij}) < R \\ 0 & \text{otherwise} \end{cases} \quad (2)$$

where C_{rel} is a cost autonomously derived from the relationship type, R is its radius of influence, and $d(p, L_{ij})$ is the distance between point p and the line segment L_{ij} connecting the two individuals. Presented with this socially augmented cost map, the planner generates a new trajectory (the red path) that avoids disrupting social interaction, even if it is slightly longer. This demonstrates how the semantic understanding provided by ReaSoN can readily be used to generate socially normative robot behavior, extending previous work in social navigation such as [33], which was constrained by simpler and less semantically rich scene models.

V. LIMITATION

Although our work establishes a solid foundation for incorporating humans and their activities into 3DSGs, it remains constrained by assumptions such as nearly static scenes and interaction contexts limited to the person’s field of view –for instance, our current approach cannot detect someone pointing to a distant object while looking elsewhere. Furthermore, our experiments were limited to synthetic scenes, but since the models used were trained on real-world data, we expect the approach to generalize and extend to more complex scenarios beyond our controlled navigation experiment.

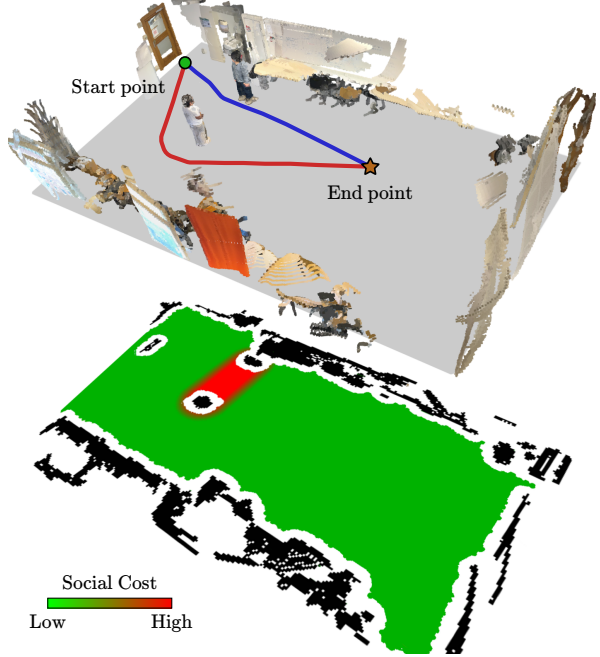


Fig. 4: Socially aware planning in a real-world scene based on the Social Scene 3D Graph obtained by ReaSoN. Without social awareness, the planner generates a trajectory that passes between two people engaged in conversation (blue), whereas incorporating social cost produces a trajectory that is longer but avoids interrupting the interaction (red).

VI. CONCLUSIONS

In this work, we introduced Social 3D Scene Graphs, a representation that we envision as a foundation for socially intelligent robots and a method, ReaSoN, to build them. By modeling humans, objects, and their interactions, this structure supports applications ranging from human-aware navigation to 3D social scene understanding. Through our benchmark, SocialGraph3D, we provide a grounding for evaluating such capabilities and through our experiments, we demonstrate how this representation improves a robot’s understanding of the environment. While our current approach is limited to static scenes, we plan to extend it to dynamic environments and pursue Sim2Real transfer by incorporating real-world scenarios into our benchmark. Moreover, our algorithm relies solely on vision and language, but incorporating other modalities such as audio could provide richer context –for example, enabling the robot to better perceive activities outside its field of view or to disambiguate human states, such as recognizing that a person near the door saying “goodbye” is likely to leave, while someone greeting has just arrived. Looking ahead, we believe that by continuously tracking and learning from human behavior in shared spaces, Social 3D Scene Graphs can support long-term personalization, allowing robots to capture individual preferences and proactively anticipate human needs.

REFERENCES

[1] C. Cadena, L. Carlone, H. Carrillo, Y. Latif, D. Scaramuzza, J. Neira, I. Reid, and J. J. Leonard, “Past, present, and future of simultaneous

localization and mapping: Toward the robust-perception age,” *IEEE Trans. on Robotics*, 2016.

[2] I. Armeni, Z.-Y. He, J. Gwak, A. R. Zamir, M. Fischer, J. Malik, and S. Savarese, “3d scene graph: A structure for unified semantics, 3d space, and camera,” *ICCV*, 2019.

[3] U.-H. Kim, J.-M. Park, T.-j. Song, and J.-H. Kim, “3-d scene graph: A sparse and semantic representation of physical environments for intelligent agents,” *IEEE Trans. on Cybernetics*, 2020.

[4] N. Hughes, Y. Chang, S. Hu, R. Talak, R. Abdulhai, J. Strader, and L. Carlone, “Foundations of spatial perception for robotics: Hierarchical representations and real-time systems,” *IJRR*, 2024.

[5] A. Dai, A. X. Chang, M. Savva, M. Halber, T. Funkhouser, and M. Nießner, “Scannet: Richly-annotated 3d reconstructions of indoor scenes,” in *CVPR*, 2017.

[6] J. Straub, T. Whelan, L. Ma, Y. Chen, and et al., “The Replica dataset: A digital replica of indoor spaces,” *arXiv*, 2019.

[7] G. Baruch, Z. Chen, A. Dehghan, T. Dimry, Y. Feigin, P. Fu, T. Gebauer, B. Joffe, D. Kurz, A. Schwartz *et al.*, “Arikscenes: A diverse real-world dataset for 3d indoor scene understanding using mobile rgb-d data,” *arXiv preprint arXiv:2111.08897*, 2021.

[8] C. Yeshwanth, Y.-C. Liu, M. Nießner, and A. Dai, “Scannet++: A high-fidelity dataset of 3d indoor scenes,” in *ICCV*, 2023.

[9] C. Zhang, A. Delitzas, F. Wang, R. Zhang, X. Ji, M. Pollefeys, and F. Engelmann, “Open-Vocabulary Functional 3D Scene Graphs for Real-World Indoor Spaces,” in *CVPR*, 2025.

[10] A. Rosinol, A. Violette, M. Abate, N. Hughes, Y. Chang, J. Shi, A. Gupta, and L. Carlone, “Kimera: From slam to spatial perception with 3d dynamic scene graphs,” *IJRR*, 2021.

[11] N. Hughes, Y. Chang, and L. Carlone, “Hydra: A real-time spatial perception system for 3d scene graph construction and optimization,” *RSS*, 2022.

[12] D. Maggio, Y. Chang, N. Hughes, M. Trang, D. Griffith, C. Dougherty, E. Cristofalo, L. Schmid, and L. Carlone, “Clio: Real-time task-driven open-set 3d scene graphs,” *RA-L*, 2024.

[13] Q. Gu, A. Kuwajerwala, S. Morin, K. M. Jatavallabhula, B. Sen, A. Agarwal, C. Rivera, W. Paul, K. Ellis, R. Chellappa, C. Gan, C. M. de Melo, J. B. Tenenbaum, A. Torralba, F. Shkurti, and L. Paull, “Conceptgraphs: Open-vocabulary 3d scene graphs for perception and planning,” in *ICRA*, 2024.

[14] A. Werby, C. Huang, M. Büchner, A. Valada, and W. Burgard, “Hierarchical open-vocabulary 3d scene graphs for language-grounded robot navigation,” in *RSS*, 2024.

[15] D. Rotondi, F. Scaparro, H. Blum, and K. O. Arras, “Fungraph: Functionality aware 3d scene graphs for language-prompted scene interaction,” *IROS*, 2025.

[16] J. Wald, H. Dhamo, N. Navab, and F. Tombari, “Learning 3D Semantic Scene Graphs from 3D Indoor Reconstructions,” in *CVPR*, 2020.

[17] S.-C. Wu, J. Wald, K. Tateno, N. Navab, and F. Tombari, “Scenegraph-fusion: Incremental 3d scene graph prediction from rgb-d sequences,” in *CVPR*, 2021.

[18] S. Zhang, A. Hao, H. Qin *et al.*, “Knowledge-inspired 3d scene graph prediction in point cloud,” *NeurIPS*, 2021.

[19] Z. Wang, B. Cheng, L. Zhao, D. Xu, Y. Tang, and L. Sheng, “Vi-sat: Visual-linguistic semantics assisted training for 3d semantic scene graph prediction in point cloud,” in *CVPR*, 2023.

[20] S. Koch, N. Vaskevicius, M. Colosi, P. Hermosilla, and T. Ropinski, “Open3dsg: Open-vocabulary 3d scene graphs from point clouds with queryable objects and open-set relationships,” in *CVPR*, 2024.

[21] D. Xu, Y. Zhu, C. B. Choy, and L. Fei-Fei, “Scene graph generation by iterative message passing,” *CVPR*, 2017.

[22] R. Pascanu, T. Mikolov, and Y. Bengio, “On the difficulty of training recurrent neural networks,” in *ICML*, 2013.

[23] A. Rosinol, A. Gupta, M. Abate, J. Shi, and L. Carlone, “3d dynamic scene graphs: Actionable spatial perception with places, objects, and humans,” *RSS*, 2020.

[24] Z. Ravichandran, L. Peng, N. Hughes, J. D. Griffith, and L. Carlone, “Hierarchical representations and explicit memory: Learning effective navigation policies on 3d scene graphs using graph neural networks,” *ICRA*, 2022.

[25] N. Gorlo, L. Schmid, and L. Carlone, “Long-term human trajectory prediction using 3d dynamic scene graphs,” 2024.

[26] C. Agia, K. M. Jatavallabhula, M. Khodeir, O. Miksik, V. Vineet, M. Mukadam, L. Paull, and F. Shkurti, “Taskography: Evaluating robot task planning over large 3d scene graphs,” *CoRL*, 2022.

[27] M. R. H. Talukder, R. I. Arnob, and G. J. Stein, “Anticipatory planning for performant long-lived robot in large-scale home-like environments,” *ICRA*, 2025.

[28] K. Rana, J. Haviland, S. Garg, J. Abou-Chakra, I. D. Reid, and N. Sünderhauf, “Sayplan: Grounding large language models using 3d scene graphs for scalable robot task planning,” *CoRL*, 2023.

[29] Y. Liu, L. Palmieri, S. Koch, I. Georgievski, and M. Aiello, “Delta: Decomposed efficient long-term robot task planning using large language models,” *ICRA*, 2025.

[30] A. Rajvanshi, K. Sikka, X. Lin, B. Lee, H.-P. Chiu, and A. Velasquez, “Saynav: Grounding large language models for dynamic planning to navigation in new environments,” *AAAI*, 2024.

[31] H. Yin, X. Xu, Z. Wu, J. Zhou, and J. Lu, “Sg-nav: Online 3d scene graph prompting for llm-based zero-shot object navigation,” *NeurIPS*, 2024.

[32] C. Mavrogiannis, F. Baldini, A. Wang, D. Zhao, P. Trautman, A. Steinfeld, and J. Oh, “Core challenges of social robot navigation: A survey,” *ACM Trans. on Human-Robot Interaction*, 2023.

[33] B. Okal and K. O. Arras, “Learning socially normative robot navigation behaviors with bayesian inverse reinforcement learning,” in *ICRA*, 2016.

[34] E. A. Sisbot, L. F. Marin-Urias, R. Alami, and T. Simeon, “A human aware mobile robot motion planner,” *IEEE Trans. on Robotics*, 2007.

[35] L. Heuer, L. Palmieri, A. Rudenko, A. Mannucci, M. Magnusson, and K. O. Arras, “Proactive model predictive control with multi-modal human motion prediction in cluttered dynamic environments,” in *IROS*, 2023.

[36] K. Fang, F. Liu, P. Abbeel, and S. Levine, “Moka: Open-world robotic manipulation through mark-based visual prompting,” *RSS*, 2024.

[37] E. Girgin, B. Gökberk, and L. Akarun, “Detection and quantification of occlusion for 3d human pose and shape estimation,” in *Pattern Recognition. ICPR 2024 International Workshops and Challenges*, S. Palaiahnakote, S. Schuckers, J.-M. Ogier, P. Bhattacharya, U. Pal, and S. Bhattacharya, Eds. Springer Nature Switzerland, 2025, pp. 368–382.

[38] A.-C. Cheng, H. Yin, Y. Fu, Q. Guo, R. Yang, J. Kautz, X. Wang, and S. Liu, “Spatialrgpt: Grounded spatial reasoning in vision-language models,” *NeurIPS*, 2025.

[39] A. Di Fabio, S. Conia, and R. Navigli, “Verbatlas: a novel large-scale verbal semantic resource and its application to semantic role labeling,” in *EMNLP-IJCNLP*, 2019.

[40] R. Navigli, M. Pinto, P. Silvestri, D. Rotondi, S. Ciciliano, and A. Scirè, “Nounatlas: Filling the gap in nominal semantic role labeling,” in *ACL*, 2024.

[41] T. Cheng, L. Song, Y. Ge, W. Liu, X. Wang, and Y. Shan, “Yolo-world: Real-time open-vocabulary object detection,” *CVPR*, 2024.

[42] A. Kirillov, E. Mintun, N. Ravi, H. Mao, C. Rolland, L. Gustafson, T. Xiao, S. Whitehead, A. C. Berg, W.-Y. Lo, P. Dollár, and R. Girshick, “Segment anything,” in *ICCV*, 2023.

[43] A. G. Howard, M. Zhu, B. Chen, D. Kalenichenko, W. Wang, T. Weyand, M. Andreetto, and H. Adam, “Mobilenets: Efficient convolutional neural networks for mobile vision applications,” 2017.

[44] T. Hempel, A. A. Abdelrahman, and A. Al-Hamadi, “Toward robust and unconstrained full range of rotation head pose estimation,” *IEEE Trans. on Image Processing*, 2024.

[45] OpenAI, “GPT-4 technical report,” *CoRR*, vol. abs/2303.08774, 2023.

[46] A. Radford, J. W. Kim, C. Hallacy, A. Ramesh, G. Goh, S. Agarwal, G. Sastry, A. Askell, P. Mishkin, J. Clark, G. Krueger, and I. Sutskever, “Learning transferable visual models from natural language supervision,” in *Proceedings of the 38th Int. Conf. on Machine Learning*, 2021.

[47] D. Duberg and P. Jensfelt, “Ufomap: An efficient probabilistic 3d mapping framework that embraces the unknown,” *IEEE Robotics and Automation Letters*, 2020.